Journal of Chromatography A, 1228 (2012) 20–30

Contents lists available at ScienceDirect

Journal of Chromatography A

journal homepage: www.elsevier.com/locate/chroma

Kinetic plot based comparison of the efficiency and peak capacity of high-performance liquid chromatography columns: Theoretical background and selected examples☆

Ken Broeckhoven, Deirdre Cabooter, Sebastiaan Eeltink, Gert Desmet*

Vrije Universiteit Brussel, Department of Chemical Engineering, Pleinlaan 2, 1050 Brussels, Belgium

ARTICLE INFO

Article history:
Available online 10 August 2011

Keywords:
Kinetic plot
Superficially porous
Gradient elution
High temperature
High pressure
Monolithic columns
Kinetic performance

ABSTRACT

The present contribution reviews the foundations of the kinetic-plot method for the direct comparison of the kinetic performance of different chromatographic support and operating modes. The method directly uses experimental data collected for a specific sample and operating condition of one's interest, and is applicable both under isocratic- and gradient-elution conditions. Experimental proof is provided for the strong relation between the kinetic performance of a given support under isocratic and gradient conditions: a material offering superior kinetic performances under isocratic conditions will remain superior under gradient conditions and vice versa provided the comparison occurs under unbiased conditions. In addition, a review is made of the recent literature using the kinetic-plot method to compare and assess the kinetic performance of high performance HPLC columns and their operation mode.

1. Physical meaning and history of kinetic plots

Since the very beginning of the modern chromatographic separation era, it has been recognized that a plot of the column void time (t_0) or the analysis time (t_R) versus the plate number (N) or the peak capacity (n_p) provides the most direct and unbiased way to compare the performance of chromatographic systems with different physicochemical properties or with different support morphologies. Calvin Giddings [1] already used such a kinetic-performance plot to compare the performance limits of LC with those of GC as early as in 1965 (Fig. 1). In 1997, Hans Poppe proposed to plot t_0/N versus N instead of t_0 versus N to obtain a more expanded view on the kinetic performance in the C-term dominated range [2]. Later, in 2006, the concept was extended by Carr and co-workers to also cover gradient-based separations [3]. In 2007, Lestremau et al. used a similar kinetic-plot approach to investigate the effect of elevated temperatures on the kinetic performance of chromatographic supports with different particle sizes, and delivered an experimental proof for the predictive properties of kinetic plots by measuring the performance on different coupled-column length systems [4].

Whereas the above mentioned authors used an iterative (and thus computer-based) strategy to construct their kinetic-plot curves, and therefore found little followers among the more practically oriented scientists in the field, it has been shown in [5] that the same curves can also be obtained without iterative procedure, by directly transforming a series of experimental plate-height curve data (H versus u_0) into a corresponding value of t_0 and N, using:

$$N = \frac{\Delta P_{max}}{\eta}\left(\frac{K_{v0}}{u_0 H}\right)_{experimental} \quad (1)$$

$$t_0 = \frac{\Delta P_{max}}{\eta}\left(\frac{K_{v0}}{u_0^2}\right)_{experimental} \quad (2)$$

where η and K_{v0} represent the mobile-phase viscosity and the u_0-based column permeability, respectively and ΔP_{max} the maximal allowable column or instrument pressure. Once N and t_0 are known, it is straightforward to also calculate some important derivative quantities such as t_R, n_p and the separation resolution R_s. This approach, referred to as the kinetic plot method, opened the way to a simpler and more user-friendly means of plotting experimental kinetic-performance data (plate-height and bed permeability), which in turn lead to a more widespread use of kinetic plots (see also Section 5) [6–19].

Variants of Eqs. (1) and (2) have recently been proposed by Carr et al. [8] and Neue [10], writing the relation between H and u_0 in

☆ The authors would like to dedicate this paper to the late Uwe Neue, who has always been a great source of inspiration and motivation and also personally appreciated the application of the kinetic plot method in HPLC. Uwe's text book and scientific papers have been essential guideposts on our journey through the field of chromatography.

* Corresponding author at: Pleinlaan 2, 1050 Brussels, Belgium.
Tel.: +32 02 629 32 51; fax: +32 02 629 32 48.
E-mail address: gedesmet@vub.ac.be (G. Desmet).

0021-9673/$ – see front matter © 2011 Elsevier B.V. All rights reserved.
doi:10.1016/j.chroma.2011.08.003

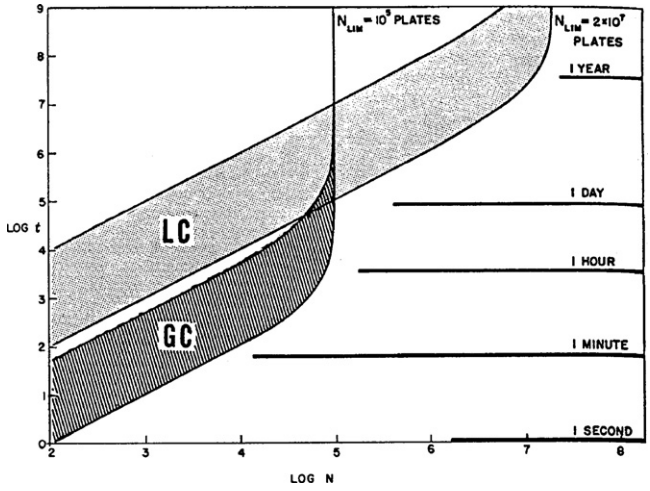

Fig. 1. First appearance of a kinetic plot in literature, comparing the kinetic-performance limits of LC and GC.
(Reprinted with permission from Ref. [1]).

the denominator of Eq. (2) in an explicit form using for example the Knox or the Van Deemter plate-height expression.

As an example, Fig. 2 compares the kinetic performance of a commercial silica monolith and a sub-2 μm particle column. The figure shows how, by using Eqs. (1) and (2), the conventionally employed Van Deemter-plot (Fig. 2a) transforms into a complementary and practically more informative plot of t_R versus N (Fig. 2b). The latter plot readily reveals that monolithic supports are superior to sub-2 μm packed bed columns when ultra-large efficiencies need to be pursued. On the other hand, when smaller efficiencies are needed, the packed bed format clearly outperforms the considered monolithic column format. This difference in behavior is essentially due to the much more open structure and the accompanying high permeability of the monolithic support ($K_{v0} = 8.0 \times 10^{-14}$ m^2 for the monolith compared to $K_{v0} = 6.3 \times 10^{-15}$ m^2 for the sub-2 μm particles), allowing to use very long columns at a sufficiently high linear velocity on the one hand, and due to the smaller diffusion distances and the better packing homogeneity of the packed bed column (leading to high separation efficiencies in relatively short columns) on the other hand [20]. Whereas the two solid line curves in Fig. 2b compare the two support types for the same 400 bar pressure (thus providing a view on the intrinsic differences originating from their different geometry), the two dashed lines compare the two materials on the basis of their proper pressure limit (respectively 200 bar for the monolithic column and 1000 bar for the particulate column). Whereas the former comparison (same pressure) is more relevant for the column manufacturers (it gives clues on the kinetic quality of the columns they are producing), the latter is more relevant for the column users (it tells them what support performs best in a given range of desired efficiencies).

The fact that Eqs. (1) and (2) lead to the same result as the more cumbersome iterative procedures used in [1–3] can be understood as follows. According to its definition, the kinetic optimum of a given support or operating condition is achieved when a given desired efficiency or peak capacity is reached in the shortest possible time, or, equivalently, when a maximal efficiency or peak capacity is reached during a given allotted analysis time. As rigorously demonstrated in Supplementary Material added to Ref. [21], this kinetic optimum is achieved if and only if the employed chromatographic support is used in a column that is precisely long enough to reach a given, user-specified pressure limit (note that each column length reaches this limit at a different flow rate). This maximal pressure-condition is automatically satisfied in Eqs. (1)

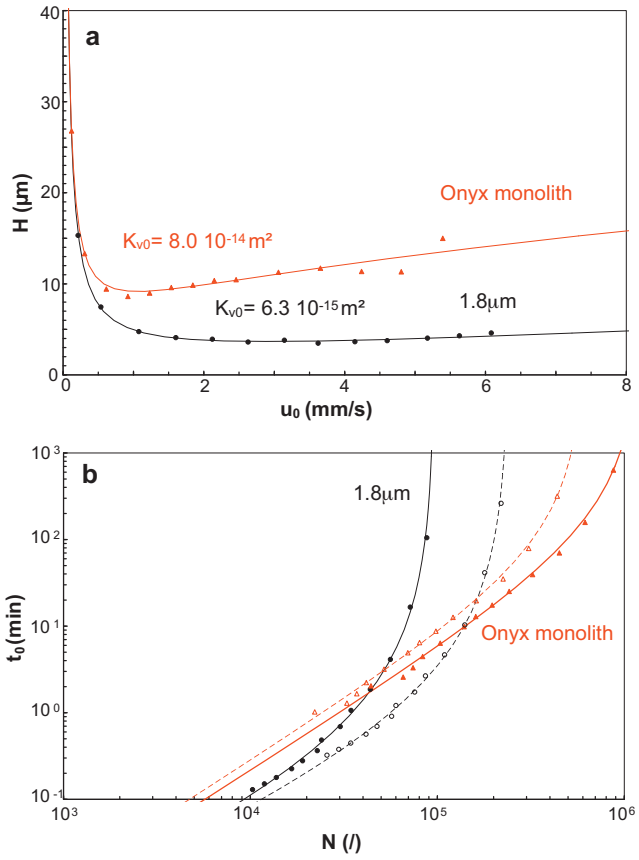

Fig. 2. Transformation obtained using Eqs. (1) and (2) of (a) experimental Van Deemter data into (b) a kinetic plot for the case of a fully porous sub-2 μm particle column (black data) and a commercial silica monolith (red data). The full line data in (b) compare both systems at identical pressure (P = 400 bar), the dashed line data compare each support type at its proper operation limit (P = 200 bar for the monolith and P = 1000 bar for the sub-2 μm column). Experimental conditions: T = 30 °C, test compound: 10 ppm methylparaben ($k \cong 2$), mobile phase: 35%/65% (v/v) ACN/H_2O for the sub-2 μm column (Agilent Zorbax SB 2.1 mm × 50 mm, d_p = 1.8 μm) and 27%/73% (v/v) ACN/H_2O for the monolith (Phenomenex Onyx 2.1 mm × 100 mm, d_{dom} = 3 μm), V_{inj} = 2 μL, λ = 254 nm. (For interpretation of the references to color in this figure legend, the reader is referred to the web version of the article.)

and (2), whereas it had to be calculated iteratively in the approaches adopted in [1–3]. Fig. 3a illustrates that the best kinetic performance is indeed always obtained at the maximal pressure end of the fixed-length kinetic plot curves [22,23]. In Fig. 3a, these are the black curves, established by measuring N and t_R at various flow rates on a column with a fixed length: it is impossible to find better combinations of efficiency and time than those situated on the kinetic-performance limit (KPL) curve (red curve) connecting the high pressure end points of all fixed-length curves. The KPL-curve envelopes the complete area of kinetic performances that can be achieved in practice with the tested material and thus represents a unique "signature" of its kinetic quality at a given pressure (P_{max}), specified by the user.

Comparing different materials or operating conditions on the basis of this "signature" automatically guarantees that the comparison occurs on a fair basis (each system is compared at its optimum, thus preventing that one system is tested under less optimized conditions than the other one) and is fully comprehensive (all possible values of N or n_p are addressed at the same time) [5,24]. The curve represents the composite effect of the band broadening and the column permeability on the kinetic performance and thus allows to assess the quality of the compromise that sometimes needs to be made between a packing with a high flow resistance but small

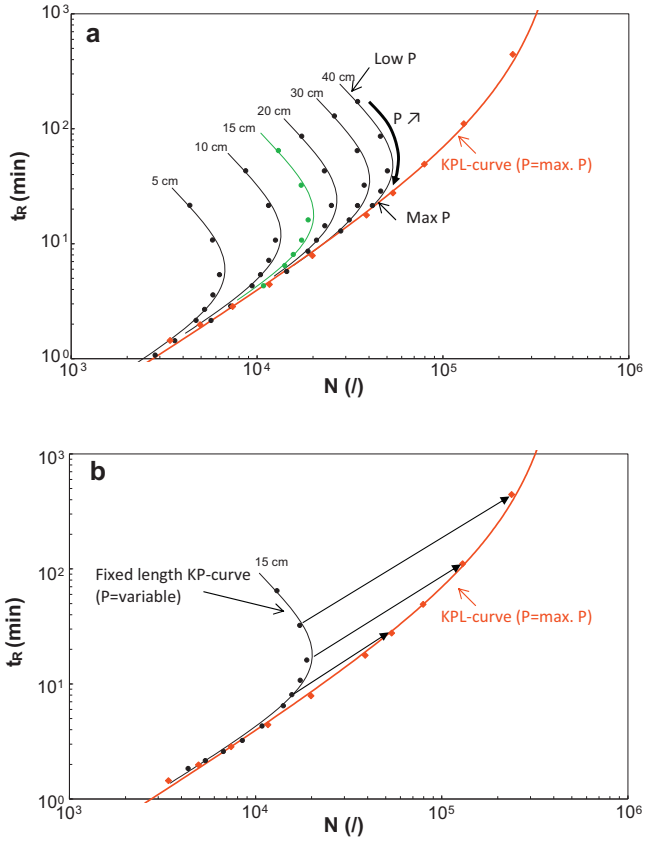

Fig. 3. (a) Experimental fixed length kinetic plot curves (black curves) on different length columns containing same particle type and enveloping KPL-curve (red curve). The arrows on the fixed length curve for $L = 40$ cm indicate the direction of the pressure change. This direction is the same for the other fixed length curves as well. (b) Direct data transformation from a fixed length kinetic plot curve into the KPL-curve as obtained when using either Eqs. (1) and (2) or Eqs. (3)–(6). Experimental conditions: $T = 30\,^{\circ}$C, test compound: 100 ppm of a pharmaceutical compound (MW = 674 with two amide functions) ($k = 10$), mobile phase: 60%/40% (v/v) ACN/0.1% formic acid, column: superficially porous (HALO 2.1 mm × 150 mm, $d_p = 2.7$ μm), $V_{inj} = 0.5$ μL, $\lambda = 254$ nm. (For interpretation of the references to color in this figure legend, the reader is referred to the web version of the article.)

band broadening (for example a packed bed column containing sub 2 μm-particles) and its opposite (for example a monolithic column with wide through-pores).

2. Unification of the isocratic and gradient kinetic plot method

Whereas Eqs. (1) and (2) are straightforward to apply under isocratic separation conditions, this no longer holds under gradient-elution conditions because in this case the (average) plate height H is more difficult to determine exactly (it requires the exact knowledge of the retention factor experienced by the analytes when eluting from the column [25,26]). In [21], it has however been shown that the use of plate heights to establish the KPL-curve is only an unnecessary detour. In fact, the KPL-curve can also be directly established using a set of t_R- (or t_0) and n_p-(or N)-data read out from a series of chromatograms produced at different flow rates on a column with a given length, and subsequently transforming these data using a length elongation factor λ to implement the aforementioned condition that the kinetic optimum is only obtained when $\Delta P = \Delta P_{max}$:

$$t_{R,KPL} = \lambda \cdot t_{R,exp} \quad (3)$$

$$n_{p,KPL} = 1 + \sqrt{\lambda} \cdot (n_{p,exp} - 1) \quad (4)$$

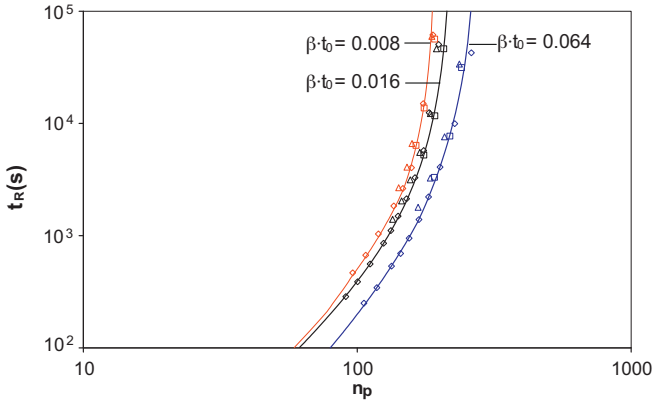

Fig. 4. Verification of the overlap of the KPL curves originating from experiments conducted in columns with different length (15 cm: ◊; 30 cm: △; 60 cm: □) for various degrees of gradient steepness ($\beta \cdot t_0 = 0.008$, 0.016 and 0.064, with $\beta = \Delta\varphi/t_G$,). The gradient programming was adapted to ensure a constant t_G/t_0 and t_{delay}/t_0 for each considered length and flow rate. Experimental conditions: $T = 30\,^{\circ}$C, test compounds: 0.02 mg/mL uracil, 0.1 mg/mL benzene, 0.05 mg/mL naphthalene and 0.05 mg/mL phenanthrene, mobile phase: $\varphi_0 = 50\%/50\%$ (v/v) ACN/H_2O and $\varphi_{end} = 100\%/0\%$ (v/v) ACN/H_2O, columns: superficially porous (HALO 2.1 mm × 150 mm, $d_p = 2.7$ μm), $V_{inj} = 1$ μL, $\lambda = 210$ nm.
(Reprinted with permission from Ref. [21]).

$$N_{KPL} = \lambda \cdot N_{exp} \quad (5)$$

$$\text{with } \lambda \text{ given by: } \lambda = \frac{P_{max}}{P_{exp}} \quad (6)$$

The subscripts "exp" and "KPL" in Eqs. (3)–(5), respectively refer to the experimental data points (as collected on a single fixed length column for a series of different flow rate) and the corresponding data points on the KPL-curve, respectively. In Eq. (6), P_{exp} is the maximal pressure reached during the gradient run and P_{max} is the reference pressure for which the KPL-curve is established (typically P_{max} would be the maximally affordable instrument or column pressure).

In physical terms, Eqs. (3)–(6) directly represent the data transformation represented in Fig. 3b, based on the fact that an experimental kinetic plot can be calculated by extrapolating data obtained on a single column length to an imaginary set of columns, each with a different length but all operated at the same pressure [27]. The major advantage of Eqs. (3)–(6) is that they hold under both isocratic- and gradient-elution conditions. This has been demonstrated mathematically and experimentally in [21]. The latter was achieved by demonstrating that, provided the data are always collected by applying the same relative mobile-phase gradient history (achieved by keeping the same ratio of t_G/t_0 and t_{delay}/t_0, with t_G the gradient time and t_{delay} the gradient delay time, i.e. the time needed for the mobile phase gradient the reach the column), always the same KPL-curve is obtained, independently of the length of the column used to collect the experimental kinetic-performance data (Fig. 4). The latter condition represents the fact that, as shown in Fig. 3a for example, there is only one KPL-curve enveloping the entire array of possible fixed length columns. On the other hand, the obtained KPL-curve can depend significantly on the actual value of the gradient steepness (especially when considering a t_R versus n_p-kinetic plot as is the case in Fig. 4), as can be noted from the fact that the different considered t_G/t_0-cases lead to different KPL-curves. This matter is further discussed in Section 4, but the observation already hints at the fact that a kinetic plot representation is also ideally suited to kinetically optimize the gradient conditions [3,16,28], for example to maximize the gradient peak capacity in a given time.

3. Relation between the kinetic performance under isocratic and gradient elution conditions

Criticism on the poor isocratic performance of certain chromatographic columns, is often countered (especially by column manufacturers) with the claim that this is of little consequence for the gradient-elution performance. This however suggests that the performance under gradient and isocratic conditions would be unrelated, which in turn would be in contradiction with the generally accepted notion that the basic band-broadening process in the gradient and the isocratic mode can be described by the same dependency on the particle diameter and mobile-phase velocity:

$$H = H_{\text{eddy}} + B(k) \cdot \frac{D_{\text{mol}}}{u} + C(k) \cdot u \cdot \frac{d_p^2}{D_{\text{mol}}} \quad (7)$$

Whereas the analytes experience only one k-value and one D_{mol}-value in the isocratic mode, they experience a whole series of different k and D_{mol}-values when travelling through the column in the gradient mode. Conceptually, this however does not change much to Eq. (7) [29]. In the gradient mode, the B- and C-constants, as well as the D_{mol}-value appearing in Eq. (7) need to be calculated by averaging them over the experienced mobile phase history, but they can anyhow be expected to remain constant for different flow rates or column lengths provided the t_G/t_0- and t_{delay}/t_0-ratio is kept constant [21], which is anyhow the "condition sine qua non" for a fair column comparison and for a valid kinetic-plot construction.

This also implies that, if one would compare an isocratic separation using a mobile phase that has a composition close to the average mobile-phase composition experienced during a gradient separation, the gradient and the isocratic mode should display very similar band broadening properties. Obviously, the gradient elution mode might additionally benefit from the peak compression effect [25,30,31]. This effect is, however, to a first approximation independent of the degree of band broadening [30], so that the advantage given to the gradient separation should be the same for all support types. In other words, the peak compression effect cannot be expected to alter the order in the performance comparison of different particle types when switching from the isocratic to the gradient elution mode.

The only case wherein this order might be significantly affected when switching from isocratic to gradient conditions occurs when comparing columns with significantly different retention behavior. From the theory of gradient elution it follows clearly [21,29,32] that the peak widths of the compound are determined not only by the column efficiency, but also by its retention factor at point of elution k_e. In addition, the achievable peak capacity (which is the best measure for column performance in gradient elution [29]) is also determined by retention times of the compounds (see also Eq. (8) further on), which are proportional to the average retention factor. Therefore, comparing columns which have largely different k and k_e-values (as could, e.g. be expected when comparing C18 packed bed and polymer monolithic columns), a good performance in gradient elution could be found for some specific samples, even when the isocratic performance is poor [33]. These cases are however outside the scope of the current contribution.

To investigate the argumentation based on Eq. (7), an experimental comparison study has been conducted wherein two fully porous and two porous-shell materials with a similar (C18) surface chemistry are compared in the gradient mode (adjusting the gradient parameters slightly in order to maintain the same elution window on all columns) and in the isocratic mode (using a mobile-phase composition so that the compound eluting near the centre of the elution window in the gradient mode elutes with about the same retention factor in the isocratic mode).

3.1. Experimental

Uracil, 2-napthoic acid, quinoline, dibenzothiopene sulfoxide, benzofuran, indene, indane, fluorene and ammonium acetate were purchased from Sigma–Aldrich (Steinheim, Germany). Acetonitrile (ACN) gradient grade for HPLC was purchased from Merck (Darmstadt, Germany) and HPLC grade water was prepared in the laboratory using a Milli-Q Advantage water purification system (Millipore, Bedford, MA, USA). Four columns with the same dimensions (100 mm × 4.6 mm) were tested: XBridge C18 3.5 μm (Waters, Milford, MA, USA), ACE C18 3 μm (Advanced Chromatography Technologies, Aberdeen, UK), Kinetex C18 2.6 μm (Phenomenex, Torrence, CA, USA) and HALO C18 2.7 μm (Advanced Materials Technologies, Wilmington, DE, USA).

All measurements were performed on a Agilent 1290 Infinity system with a binary pump, a diode array detector with a MaxLight cartridge cell (V = 1 μL, 10 mm path length), an autosampler, a temperature-controlled column compartment (set at 25 °C) and operated with Agilent Chemstation software. The mobile phase passed through the built-in 3 μL mobile phase preheater before entering the column. Absorbance values were measured at 210 nm with a sample rate of 40 Hz and the peak widths were determined at half height. Retention times and column pressure drops were corrected for the extra column contributions. Samples consisting of 0.04 mg/mL uracil and 0.10 mg/mL for each of the other compounds were dissolved in 50%/50% (v/v) ACN/H_2O. The injected sample mixture volume was 1 μL and the system dwell volume was determined (using the procedure described in [34]) to be 120 μL.

The isocratic experiments were performed using uracil as t_0-marker and dibenzothiopene sulfoxide to determine the column performance. This compound elutes halfway the separations in gradient mode, yielding the most representative 'average' retention behavior of the considered sample in gradient elution. The mobile phase composition ϕ_{iso} (consisting of ACN/10 mM ammonium acetate buffer) was adjusted for each column type in such a way that the compound eluted with a retention factor $k \cong 7$ (see Table 1), i.e. the average of the retention factors of the first and last eluting compound in the gradient runs (see further on).

To determine the separation performance in gradient elution, a constant ratio of gradient time t_G over column dead time t_0 was maintained ($t_G/t_0 = 12$) for all columns and flow rates, followed by an isocratic hold equal to t_0 at the final mobile-phase concentration. The initial (ϕ_0) and final (ϕ_{end}) mobile-phase compositions of the gradient were adjusted for each column type independently to yield $k \cong 2$ for the first (2-napthoic acid) and $k \cong 12$ for the last compound (fluorene) in the sample (see Table 1), following an approach recently presented in [35]. The separations on the different columns were thus compared for the same k-based elution window. For the column pressure, the highest value encountered during the gradient run was taken (corresponding to the mobile-phase composition having the highest average viscosity).

For both the isocratic and gradient runs, the peak capacity n_p was calculated using the following equation [21,36]

$$n_p = 1 + \sum_{i=1}^{n} \frac{t_{R,i} - t_{R,i-1}}{4 \cdot \sigma_{t,i}} \quad (8)$$

with σ_t the peak standard deviation, $t_{R,i}$ the retention time of the ith compound, where $t_{R,0} = t_0$ and n the number of compounds in the sample. Starting from the definition of separation resolution R_s between two peaks ($R_s = (t_{R,i+1} - t_{R,i})/(4{\cdot}\sigma_t)$), it is clear that peak capacity represents the theoretical number of equally spaced peaks that can be separated with a certain resolution ($R_s = 1$ if peak width is established at $4{\cdot}\sigma_t$). For the isocratic experiments, Eq. (8) reduced to $n_p = 1 + (t_R - t_0)/(4{\cdot}\sigma_t)$, whereas for the gradient performance, all six peaks ($n = 6$) were used to determine the peak capacity. On each

Table 1
Column, retention and mobile phase parameters at a flow rate F = 1 mL/min (column dimensions: 4.6 mm × 100 mm).

Column	d_p	Type	t_0 (s)	ϕ_{iso} (v% ACN)	k_{iso}	ϕ_0 (v% ACN)	ϕ_{end} (v% ACN)	k_1	k_{last}
Xbridge	3.5	FP[a]	65.1	31.2	7.1	14.0	70.0	2.0	11.7
ACE	3.0	FP[a]	65.4	33.6	7.2	16.0	75.0	1.9	11.7
Kinetex	2.6	SP[b]	57.2	32.3	7.2	13.5	68.5	1.9	11.8
HALO	2.7	SP[b]	54.3	33.2	7.2	12.5	73.5	1.9	11.8

[a] FP = fully porous.
[b] SP = superficially porous.

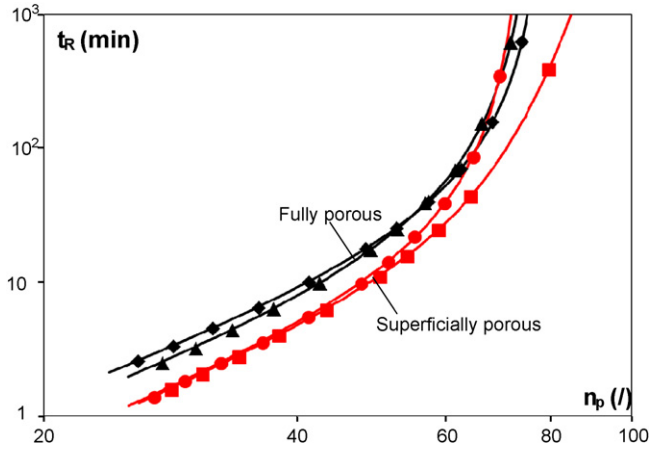

Fig. 5. Comparison of the kinetic-performance limit of columns packed with fully porous (black curves: (♦) Xbridge and (▲) ACE) and superficially porous particles (red curves: (●) Kinetex and (■) HALO) in isocratic elution. Experimental conditions are given in Section 3.1 and Table 1). (For interpretation of the references to color in this figure legend, the reader is referred to the web version of the article.)

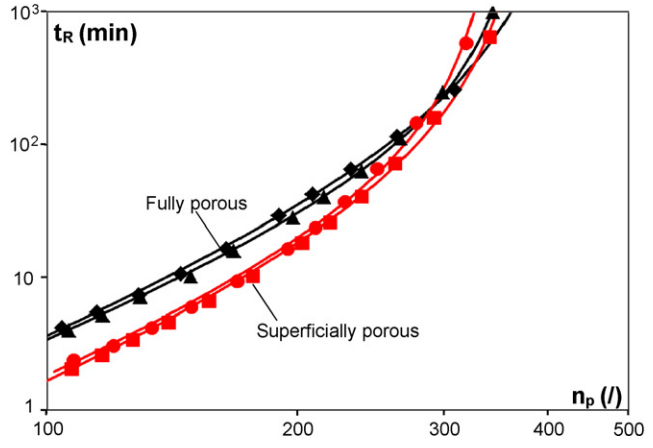

Fig. 6. Comparison of the kinetic-performance limit of columns packed with fully porous and superficially porous particles in gradient elution. Same symbols as Fig. 5. Experimental conditions are given in Section 3.1 and Table 1.

column, the performance was measured at 11 different flow rates (ranging between 0.25 mL/min and 4 mL/min), ensuring that the column pressure drops were within the limits set by the manufacturers (i.e., 400 bar for the columns with fully porous particles and 600 bar for the superficially porous particles).

3.2. Results and discussion

Fig. 5 compares the isocratic kinetic performance of the four considered particle types: the two fully porous ones and the two superficially porous ones. Fig. 6 does the same but for gradient elution conditions. In both cases, the kinetic performance is reported as a total analysis time versus the peak capacity, as this is anyhow the most convenient one for the gradient elution case. To compare all material types on the same basis, the same maximum column pressure (400 bar in the presently considered case) was used for all of them, regardless of the fact that some of the particle types have a higher operating limit (600 bar for most of the superficially porous columns (with d_p > 2 μm), and even 800 bar for the 2.1 mm ID Kinetex columns).

Comparing the isocratic (Fig. 5) and the gradient (Fig. 6) kinetic performance of the different particle types, a striking similarity between the two operating modes can be noted. In both cases, the superficially porous particles clearly outperform the fully porous ones over most of the accessible n_p-range, and also the subtle differences between the two different particle types belonging to the same group of materials (superficially porous or fully porous) are largely maintained when switching from the gradient to the isocratic elution mode and vice versa. It could be noted that the use of peak capacity is not ideally suited for isocratic experiments as a quantitative measure for column performance, since the peak width of only one component is considered for the entire elution range. This however only has a quantitative effect on the observed peak capacities and therefore does not influence the qualitative performance comparison of the different columns. Fig. S-1 in the Supplementary Material illustrates this with a comparison of the columns using a plot of t_R versus N, and shows that the same relative kinetic performance between the columns is found.

For the fully porous columns, the ACE column yielded a better kinetic performance than the Xbridge column for t_R > 0.5 h in isocratic elution and t_R > 1.5 h in gradient mode. This behavior is expected from the difference in particles size (3 μm versus 3.5 μm), as discussed in more detail in Section 5.2 (Fig. 10). When comparing the superficially porous particles, the tested HALO column provided a better performance in the B-term dominated part of the KPL-curve (high n_p-end) in both elution modes (as previously observed [37]), whereas the difference in performance between the two tested columns was negligible around the optimum velocity and in the C-term regime (low n_p-end). To illustrate that the superior performance of the superficially porous particles is not only a consequence of the small difference in particle size, Fig. S-2 in the Supplementary Information compares the performance of fully porous particles with three different particle sizes [34] with that of the HALO column presented in Fig. 6. Even compared to smaller particles (d_p = 1.7 μm), the superficially porous particles (d_p = 2.7 μm) exhibit a better kinetic performance, showing that not only particle size can be responsible for the difference in kinetic performance observed in Fig. 6.

4. Influence of the test conditions on the obtained kinetic-performance limit curve

Just as a fair comparison based on a Van Deemter curve should preferentially occur using the same compounds and the same mobile phase (and/or the same retention factors), this also holds for a kinetic-plot based comparison. This is especially true when considering kinetic plots involving one or more parameters that depend heavily on the retention factors of the compounds, such

as the total residence time t_R or the peak capacity n_p. For the latter, a number of different possible definitions co-exist in literature [38]. Roughly, they can be divided in t_R-based peak capacities (end of elution window determined by retention factor of last eluting compound) and t_G-based peak capacities (end of elution window determined by breakthrough of end of gradient profile). Depending on the purpose of the kinetic plot comparison, one type is to be preferred over the other and vice versa (see also Section 5).

Kinetic plots based on t_0 and N are less prone to differences in retention factor, and therefore are to be preferred when trying to assess the intrinsic kinetic properties and packing quality of a column. However, plots based on t_0 and N are sensitive to the retention factor via the general dependency of N on k (cf. the appearance of k in the general plate height expression of packed beds [39]). All possible kinetic-plot curves furthermore also directly depend on the employed mobile phase via the appearance of the viscosity in Eqs. (1)–(3), albeit in a hidden form in the latter case. However, this dependency on the mobile-phase viscosity can, if desired, easily be omitted by using a single dummy-value for the viscosity.

When columns or conditions with widely differing retention properties are to be compared, the use of a constant mobile-phase composition or gradient profile could lead to widely differing retention factors. In this case, given the significant impact the value of k can have on the observed efficiency (and especially on the observed peak capacity) it might be preferable to adapt the mobile phase (gradient) for each different system individually, so that they are all compared under the conditions of (approximately) equal retention factors (as illustrated in Section 3 and Ref. [35]). This especially holds when t_R is plotted versus a t_R-based peak capacity, as this type of plots are very sensitive to the k-value of the last eluting compound. In some extreme cases (for example when comparing a non-porous and a fully porous particle column, or when comparing a reversed-phased and a HILIC-system), some radically different mobile phase compositions will have to be employed to pursue conditions producing similar retention windows on the different systems. In such cases, it cannot be excluded that the selection of the sample compounds can lead to a bias, favoring or disfavoring some of the tested columns or operating conditions more than the others. A possible way out of this problem is to select a sample containing a good variety of the typical compounds one expects in a given application, and optimize the mobile phase (gradient) of each considered system individually. In this way, each different system is represented by its best possible performance, providing a suitable and practically relevant comparison basis. As an alternative solution, Zhang et al. [40] proposed determining the value of the solvent strength parameter S for the different compounds in the sample and applying the same sample based gradient steepness (S_{av} $[\phi_{end} - \phi_0]$ t_0/t_G) with a fixed ϕ_0 for both columns.

Next to the considerations one needs to make when establishing gradient kinetic plots (requiring that all measurements are conducted for the same t_G/t_0- and t_{delay}/t_0-ratio's so that the compounds always have the same retention factor), special attention should also be paid to the elimination of extra-column band broadening (ECBB) and pressure-drop sources. As described by Heinisch et al. [41], this can relatively easily be done for isocratic separations. For gradient separations, the correction for extra-column band broadening is more tedious because the bands may undergo a different focusing and defocusing effect at the column inlet and outlet, so that the ECBB one would measure via the classical method (replacement of column via a union piece) is no longer representative for the true ECBB in gradient elution. Indeed, the isocratic correction expression (see, e.g. Eq. (6) in [41] or Eq. (23) in [21]) overestimates the contribution of the ECBB since it lumps both the pre- and post-column contributions. Whereas the latter is independent of the elution mode (isocratic or gradient), the contribution to the observed peak width of the former is much smaller in gradient elution due to the focusing effect on the front of the column (where the retention is very high at the start of the gradient). Both contributions should therefore be considered separately, but this requires elaborate procedures. The only elegant solution for the extra-column band-broadening problem hence consists of reducing it as much as possible and measuring the data so that they need as little correction as possible (preferably the column peak variance should be $\gg$10 times the extra-column variance).

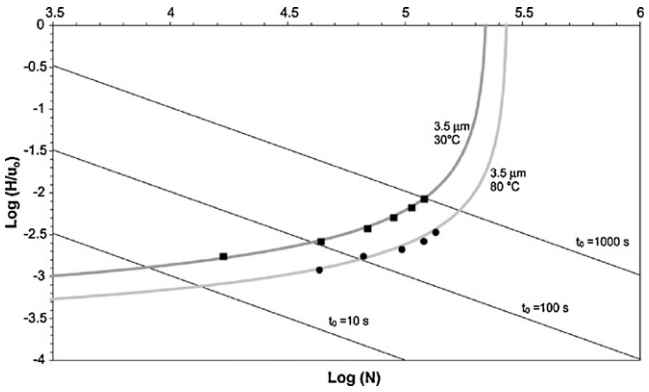

Fig. 7. Comparison of the kinetic-performance of 3.5 μm Stable Bond Zorbax C18 at 30 °C and 80 °C for the isocratic elution of phenol with a 40%/60% (v/v) ACN/H_2O mobile phase (full lines = theoretical prediction, solid data points = experimental verification).
(Reprinted with permission from Ref. [4]).

When kinetic plots are used to select the best possible chromatographic system (i.e. particle size, flow rate, column length, etc.), and when this would turn out to have significantly different length than that of the column used to generate the kinetic plot data, it is important to know the conditions wherein this column length extrapolation can be made without introducing a significant error (when kinetic plots are used to assess the column packing quality this is less relevant because the length extrapolation occurs for all different tested packing materials in the same way, i.e., by assuming a length-independent plate height). Unfortunately, the increasing operating pressures that accompany the use of longer columns, introduces several, often non-linear, effects on column performance and analyte retention.

An increase in operating pressure typically results in an increase in retention [42,43] (except in some rare cases [44]). In addition, the mobile-phase viscosity increases (η) with increasing pressure and as a result the diffusion coefficients (D_{mol}) decrease. The equations underlying the kinetic-plot method (see, e.g. Eqs. (1) and (3)) however assume that column performance (H), retention (k) and mobile-phase viscosity are independent on column length and hence also of column pressure. In addition, heat is generated inside the column due to viscous heating, causing both radial and axial temperature gradients that in turn effect D_{mol}, k, η and H in an inverse way than pressure. For systems operating at moderated pressures (<400 bar) or when using capillary columns, these effects are in general small and the experimental performance agrees almost perfectly with the kinetic-plot predictions [4], as can be seen from Fig. 7. At higher operation pressures the viscous-heating effects become more pronounced, although the amplitude of errors on the kinetic plot predictions depends on the thermal environment in which the columns are operated. In a study by Cabooter et al. [45] it was found that for a near-adiabatic system (still air oven) there was an average error of 3% (max. 9%) between predicted and measured values, while an average error of 8% (max. 13%) was found for a near-isothermal system (forced air oven). A detailed discussion concerning the effect of the length of the column in which the experimental column-performance data were obtained on the

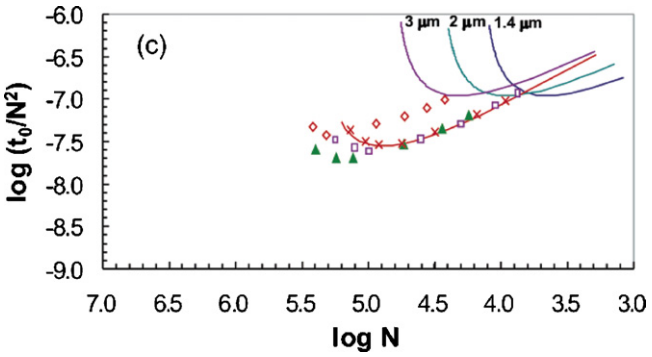

Fig. 8. Comparison of the performance of packed bed columns with different particles sizes (assuming $\eta = 4.6 \times 10^{-4}$ Pa s, $\phi_0 = d_p^2/K_{t0} = 700$, $D_{mol} = 2.22 \times 10^{-9}$ m^2/s, and h calculated using the following Knox equation: $h = 0.65\nu^{1/3} + 2/\nu + 0.08\nu$) with different types of silica-monolithic columns (symbols) for a maximum pressure P_{max} of 1000 bar.

(Reprinted with permission from Ref. [6]).

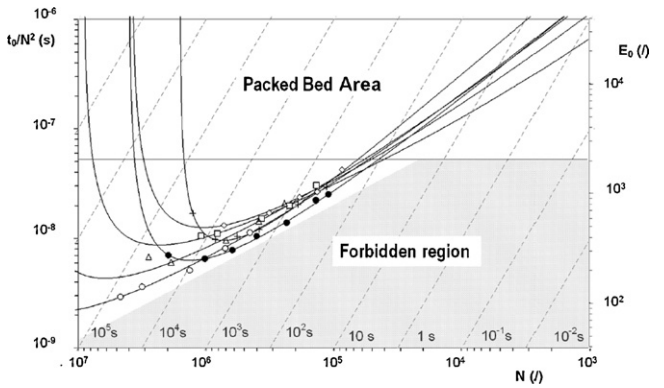

Fig. 9. Compilation of a set of t_0/N^2 versus N-curves for a variety of different monolithic silica capillary columns, showing the existence of a so-called "forbidden region" that can only be penetrated if one would succeed in making silica monoliths with smaller domain sizes without loosing the degree of homogeneity of their large domain size counterparts.

(Reprinted with permission from Ref. [50]).

obtained KPL-curve can be found in the Supplementary material of Ref. [21].

5. Use of kinetic plots in literature to compare different support types and operating conditions

Depending on whether one is rather a column producer or a column user, kinetic plots can be used for either (i) column quality evaluation (see Section 5.1) and (ii) selection of the most suitable support type and/or operating conditions (see Section 5.2). An excellent overview of all the different recent improvements in column technology and the range of separation applications they are most suited for has been given by Guillarme et al. [11].

5.1. Intrinsic column quality evaluation

For application (i), kinetic plots should be used that are minimally affected by the actual retention factors of the analytes (for example using t_0 instead of t_R and using N or a t_G-based peak capacity to quantify the separation efficiency instead of a t_R-based peak capacity). If desired, a magnified view of the difference between the kinetic plot curves corresponding to the different tested columns can be obtained by plotting the data as t_0/N^2 versus N instead of as t_0 versus N. The former type of plot furthermore offers the additional advantage that it produces curves that go through a minimum at exactly the same velocity as the corresponding Van Deemter-curve. Plotting the N-axis in the reverse direction furthermore also puts the B-term and the C-term dominated parts of the curve in the same position with respect to the curve minimum as in a Van Deemter-plot. t_0/N^2 versus N plots have for example been used by Hara et al. [6,46] to evaluate the kinetic performance of a series of newly synthesized silica-monolithic columns (Fig. 8).

The plot in Fig. 8 shows that this second-generation monolithic silica capillary columns reported by Hara et al. yield better kinetic performance than a particulate column packed with 2 μm particles as soon as efficiencies of more than 25,000–30,000 theoretical plates are needed [5,47].

Recently, insights obtained using the kinetic-plot method inspired Miyamoto et al. [48] to produce ultra long monolithic silica-C18 capillary columns (1130–1240 cm) yielding record efficiencies of over 1,000,000 theoretical plates. A kinetic plot analysis was also used to examine the chromatographic performance of a new type of silica rod column, indicating that the monolithic columns operated at 300 bar can provide faster separations than a column packed with totally porous 3-μm particles operated at 400 bar in a range where the number of theoretical plates (N) is greater than 50,000 [49].

The kinetic-plot method also allowed to demonstrate the existence of an apparent "forbidden region" [50] that can only be penetrated if one would succeed in making silica monoliths with smaller domain sizes without loosing the high degree of homogeneity of their large domain size counterparts (Fig. 9). In the history of monolithic silica column production, it appeared that all attempts to reduce the domain size were unfortunately also accompanied by an increase of the heterogeneity, leading to an accumulation of the kinetic plot curves (instead of moving rightward and penetrate the forbidden zone). In addition, theoretical calculations seem to suggest that all attempts to reduce the feature or domain size of LC supports will eventually face a lower limit band of kinetic performances that can no longer be surpassed significantly by further decreasing the domain size, thus confirming the existence of such a forbidden zone [51]. The work of Hara et al. [6,46] however shows that a careful optimization of the synthesis conditions can produce structures that allow to gradually penetrate this zone.

The kinetic performance of polymer-based monolithic columns has been assessed by Causon et al. [52], and was used to propose new directions for the column development. Horie et al. used the kinetic-plot method to compare the performance of HILIC silica monoliths with packed HILIC columns [53,54]. They found a kinetic performance that was much higher than conventional 5 μm particle-packed HILIC columns.

Using a similar plot format, Billen et al. [55] were able to relate the presence of particle fines in sub-2 μm high performance columns to an inferior kinetic performance. The effect of the particle fines became especially apparent using a so-called reduced kinetic plot, wherein both the x- and y-axis are made dimensionless so that the effect of any difference in average particle size (which is inevitable when particle fines are present) is excluded. To obtain a dimensionless y-axis, it suffices to multiply the t_0/N^2 value with the ratio of $\Delta P/\eta$, so that one readily obtains Knox' separation impedance parameter [10,56]:

$$E_0 = \frac{\Delta P_{max}}{\eta} \frac{t_0}{N^2} \quad (9)$$

A dimensionless x-axis can be obtained by plotting the ratio of N_{opt}/N instead of the purely plotting N [55].

In a subsequent comparison study of commercial sub-2 μm ad 3 μm columns, also using the same dimensionless format of a plot of E_0 versus N/N_{opt}, a correlation between a narrow particle size distribution and a superior kinetic performance was again obtained

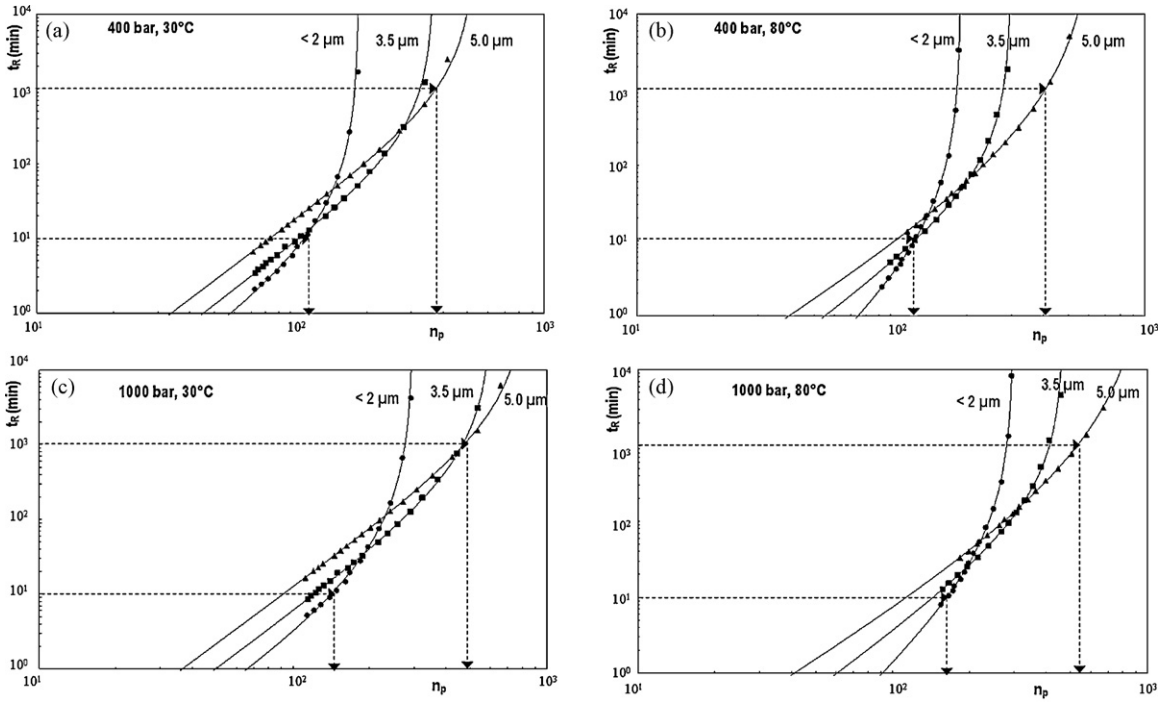

Fig. 10. Plot of t_R versus n_p obtained under isocratic elution conditions for different particle sizes (sub-2 μm (●), 3.5 μm (■) and 5 μm (▲)) and for different combinations of pressure and temperature: (a) T = 30 °C and ΔP = 400 bar; (b) T = 80 °C and ΔP = 400 bar; (c) T = 30 °C and ΔP = 1000 bar and (d) T = 80 °C and ΔP = 1000 bar. t_R-values relate to compounds eluting at k = 10.

(Reprinted with permission from Ref. [60]).

[57]. In a recent study, involving 7 different reversed-phase particle types, again a good correlation between the particle size distribution (PSD) of the particles and the typically employed "goodness of packing"-parameters was observed. The relative standard deviation of the PSD of the tested particles ranged between 0.05 and 0.2, and in this range, a near linear relationship between the A-term constant, the h_{min}-value and the minimal separation impedance E_0 was found [58].

5.2. Selection of the most suitable chromatographic system

Being a column user rather than a column manufacturer, one would mostly be using kinetic plots to select the kinetically most advantageous chromatographic system (support type, stationary phase type, mobile phase propagation method, extra-column configuration, etc.). In this case, it is preferable to use test compounds that are as relevant as possible for the type of applications one is mostly running [13,15,18,19,35,37] and to select a kinetic plot type containing the practically most relevant parameters, preferring t_R over t_0 to quantify the separation speed and preferring a t_R-based peak capacity over the t_G-based peak capacity or the plate number N to quantify the separation efficiency. Using a t_R-based peak capacity, the resulting kinetic plot curve can depend significantly on the employed gradient slope and starting composition, thus offering the possibility to kinetically optimize these parameters [12,28].

When it specifically comes to selecting a system offering the best resolution (R_s) between a given critical pair, it is even possible to directly make a plot of t_R versus R_s [19,24].

Finding the optimal particle size for a given range of desired efficiencies has probably been one of the most frequently adopted applications of the kinetic-plot method in the past few years [3,21,36,59–61]. In each case, observations were made that are fully similar to those shown in the different panels of Fig. 10, compiling results on different C18-columns for the isocratic elution of propylparaben (k = 10). Fig. 10 shows that, when employed at the same pressure limit, small particles are to be preferred in the range of relatively easy separations (range of small N), whereas large particles (3 and even 5 μm) still yield better performances when very high efficiencies are needed. A fully similar observation is made under gradient elution conditions, as can for example be witnessed from Fig. 5 of [21].

Recently, several studies have assessed the difference in kinetic properties between fully porous and porous-shell particles [13,16,35,40,62]. Fekete et al. [62] found that novel sub-2 μm superficially porous particles, which could be operated up to 1000 bar, exhibited a significantly higher kinetic performance than fully porous sub-2 μm particles (at the same pressure limit) and 2.7 μm superficially porous particles (at 600 bar pressure limit) for both small (estradiol, MW = 272 g/mol) and large (polypeptides and proteins, 4.1–66.3 kDa) molecules in isocratic elution, over the entire range of analysis times. Comparing the fully porous sub-2 μm columns at 1000 bar with 2.7 μm superficially porous particles at 600 bar, the results described in literature are however not consistent. Where Zhang et al. [40] found that the sub-3 μm superficially porous particles (600 bar) slightly outperformed the sub-2 μm (1000 bar) for relatively small MW pharmaceutical compounds (≈500 g/mol), the opposite trend was observed in the study by Fekete et al. [62] (MW = 272 g/mol). In the latter study however, the superficially porous particles exhibited a better performance for the large MW compounds, which is in turn inconsistent with the results found by Ruta et al. [16], who found better kinetic performance for the fully porous particles for all flow rates around and above the optimum mobile-phase velocity. These discrepancies however might in part be the result of column-to-column variations in performance and permeability, since only one column of each type was tested. In addition, in another study a strong difference in performance for columns from the same manufacturer but with a different inner diameter was observed [13]. Also, the compounds and conditions used to determine the KPL were different in the various studies, which might in part influence the comparison

(as discussed further on). Nevertheless, it was clear from these studies and several others [13,35] (see also Section 3 and Figs. 5 and 6) that superficially porous particles outperform fully porous particles when compared at the same operating pressure. This also shows that expanding the allowable operating pressure of superficially porous particles to those of sub-2 μm particles (i.e., 1000 bar and above) would result in previously unsurpassed separation performance (as illustrated further on).

Another obvious application of kinetic plots is their use to assess the true advantages of monolithic versus packed bed columns. As shown by Kobayashi et al. [63], compiling an extensive set of monolithic and packed bed column data showed that monolithic columns offer the distinct advantage to break through the Knox and Saleem limit delimiting the kinetic-performance region of packed bed columns, in full agreement with the theoretical expectations [20] and other experimental studies [64]. However, the current domain sizes are still too large to break through the Knox and Saleem limit in the practically most interesting range of separations requiring 10,000–30,000 theoretical plates [63,64].

Kinetic plots are also suited to quantify the potential advantage of high-temperature LC. Using a theoretical kinetic plot, complemented with experimental data collected using acetophenone and phenol separations on 3.5 μm Stable Bond Zorbax columns with different (coupled) lengths (see Fig. 7), Lestremau et al. [4] demonstrated that the gain one can expect by moving from a 30 °C to an 80 °C is of the order of about a factor of 2–2.5 if both conditions are compared for the same achieved efficiency. This gain factor is clearly large and significant, but not as large as the factors of 10–20 that are sometimes claimed. The latter is due to the fact that in a kinetic plot the two systems are always compared on the basis of an optimized length, whereas in a pure one-to-one comparison the column length is usually only optimized for one condition but not for the other. Lestremau et al. [4] also considered larger temperature increases: considering a temperature increase from 30 °C to 120 °C, their kinetic-plot analysis predicted a gain factor of about 3–4. Similar data were obtained in [65] studying three different high-temperature stable columns (Zirchrom-PBD, Zirchrom-Carb and Nucleodur Gravity), adjusting the mobile-phase composition such that the retention coefficients did not vary significantly from temperature to temperature. In this paper, it was concluded that the kinetic gain factor that can be expected over most of the C-term dominated range largely parallels the decrease in viscosity of the mobile phase induced by the temperature increase, agreeing very well with the above mentioned gain factors of 2–2.5 (for operations at 80–90 °C) and 3–4 (for operations at 120 °C). Similar observations were made by Louw et al. for typical HILIC-separation conditions [17]. In gradient elution the benefits of operating at elevated temperatures were demonstrated by Guillarme et al. [12], who found that in increase from 30 °C to 90 °C resulted in a 20–30% higher peak capacity for a constant gradient time or a 2–3-fold decrease in analysis time for the same peak capacity, i.e. roughly the same as found in isocratic elution.

Another classic application of kinetic plots is the illustration of the effect of an increased inlet pressure [4,5,8,21,24,59,64,66–68]. In all cases, it was found that the effect of pressure is most beneficial for separations requiring large peak capacities. This is also what is observed in the example shown in Fig. 11, showing the effect of the adopted ΔP_{max}-value on the KPL-curve for the case of a mixture of commonly encountered waste water pollutants separated in gradient elution (k = 2–12) on a Kinetex 2.6 μm column (conditions described in Section 3). The KPL-curve shifts to the right with increasing ΔP_{max}, providing better separation performance and/or shorter analysis times. The gain for fast (low efficiency) analyses is limited: e.g. to reach a separation performance of n_p = 120, a 2.5-fold increase in pressure (400 bar versus 1000 bar) only results in a decrease of analysis time of around 25% (2.2 min versus 3 min). In the high efficiency region however (e.g. for n_p = 250), increasing the operating pressure by the same factor, would reduce the required analysis time by more than factor of 3 (20 min versus 65 min).

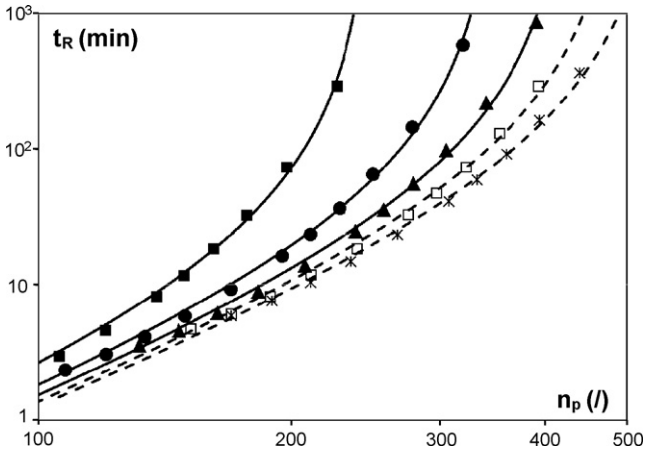

Fig. 11. Effect of the maximum allowable operating pressure on the KPL-curve for the Kinetex column in gradient elution: ΔP_{max} = 200 bar (■), ΔP_{max} = 400 bar (●), ΔP_{max} = 600 bar (▲), ΔP_{max} = 800 bar (□), ΔP_{max} = 1000 bar (×). Dotted lines and symbols represent cases where the operating pressure is higher than the pressure limit of the columns such as they are presently commercially available (for an ID of 4.6 mm). Same experimental conditions as Fig. 6.

In [64,65], it has been remarked that the beneficial effect of elevated pressures (essentially improving the performance at high efficiencies) is complementary to that of high temperatures (essentially improving the performance in the low efficiency range) [64,65].

Kinetic plots can also be used to assess the effect of the extra-column tubing and the injector and detector volume on the over-all kinetic performance. In [41], this was done for two commercial high temperature-ultra high-pressure instruments. The authors distinguished between "column-only" and "total instrument" kinetic-performance plots. It was shown, that the gain in separation speed is more strongly affected by the extra-column dispersion and pressure drop in the high-temperature range than it is in the low one. It was also pointed out that, in order to get the most out of a high-temperature operation, it seems much better to prefer an instrument offering a higher maximum flow-rate rather than a higher maximum pressure (some instruments require that this trade-off is made).

Optimizing extra-column effects using kinetic plots has recently also been done by Xu and Weber for the optimization of the dimensions of an open tube or packed capillary following the separation column, and acting as a post-separation reactor or simply as a connection tube to a mass spectrometer [69]. They found that, for very fast separations (t_0-time in the order of 10 s), extremely narrow tubes (order of 5 μm) are needed (even when packed with submicron particles). The use of higher temperatures alleviates the problem, allowing the use of larger ID connection tubing.

As they compare chromatographic performances in terms of the universal currencies "time" and "efficiency" or "peak capacity" or "resolution", kinetic plots also allow to directly compare different separation methods based on different mobile-phase propagation methods. Fekete et al. [70] have used the kinetic plot method to compare the kinetic-performance limits of (U)HPLC with those of capillary electrophoresis (CE) and shear-driven chromatography (SDC). Eeltink et al. [27] compared the kinetic-performance limits of HPLC and CEC on capillary columns packed with spherical particles, silica and polymer monoliths. They found that the CEC-mode lead to significantly faster separations than the HPLC-mode in the C-term dominated regime. The maximal efficiencies that can

be achieved in the CEC-mode on the other hand were significantly smaller than in the HPLC-mode.

A significant amount of work has also been done to investigate the effect of the employed test analytes on the observed kinetic performance. Using pharmaceutical compounds with a molecular weight in the range of 300–700 as representative real-life analytes, de Villiers et al. [18] demonstrated that differences in the optimal kinetic performance of a chromatographic system can be observed compared between data obtained for customarily used test compounds such as alkylbenzenes or parabenes, thus highlighting the importance of using real-life samples to perform kinetic evaluations for optimization purposes. They found that the optimal particle size/maximum pressure combination depends strongly on the analyte under investigation, with the beneficial range of efficiencies for small particles shifted towards higher plate numbers for drug molecules compared to molecules with a MW in the sub 200-range. In other words, the fast separation of drug molecules would benefit more from the availability of small particles than is the case for very small MW compounds. This is in full agreement with the relation between the molecular diffusion coefficient of the analytes and the corresponding optimal particle diameter [59,71,72]. This was as also pointed out by Guillarme et al. [12], who came to the same conclusion regarding the effect of MW on kinetic performance and the importance of choosing relevant test compounds for the kinetic optimization. de Villiers et al. [18] further demonstrated that the pH of the mobile phase plays a crucial role in determining the kinetic performance of pharmaceutical compounds. The importance of the pH-conditions was recently confirmed considering drug-molecule samples [19]. As previously mentioned, using the kinetic plot method, Fekete et al. showed that the advantages of superficially porous particles become more pronounced for larger MW compounds [13,62]

Whereas the majority of the results has been obtained in the reversed-phase mode, kinetic plots have also been used to study HILIC-mode columns. Chauve et al. [61] compared the kinetic performance of different types of sub-2 μm particles with that of 2.7 μm superficially porous particles with different allowable maximum operating pressures in HILIC mode. They found that, as the backpressure is always much lower in HILIC compared to reversed phase HPLC, the advantages of the superficially porous particles (i.e. the much lower permeability) in HILIC mode were not so significant as in HPLC. Louw et al. [17] used kinetic plots in HILIC separations to study the effect of temperature on performance and they compared the predictions with experiments on coupled columns. They found a significant gain in analysis time without loss of efficiency operating columns at 80 °C instead of 30 °C. They also showed the advantages of using long columns in HILIC in combination with elevated temperatures for separation of pharmaceutical compounds.

The kinetic-plot method has recently also been applied to characterize the performance of ion-exchange columns by Causon et al. [7,28] and to predict performance across a wide range of conditions. They validated the kinetic-plot predictions in isocratic elution by performing separations using coupled columns and found that their prediction errors were below 15%, despite poor column performance and column-to-column reproducibility [7]. Using isocratic retention and performance data, they preformed numerical predictions of the performance in gradient IC elution. For a gradient elution analyzing 14 typical organic and inorganic anions, a good agreement in efficiency with the predicted values was found [28]. It also appeared from the theoretical study that increasing separation temperature provides only a moderate improvement in the peak capacity in IC.

Popovici and Schoenmakers [73] presented kinetic plots for size-exclusion chromatography using polystyrene as a sample compound and THF as the mobile phase. Because of the very high-reduced velocities encountered in ISEC with only a very slow accompanying increase of the plate height, the kinetic plots differ significantly from those commonly observed in HPLC. It was found that fast separations in size-exclusion chromatography are not as unfavorable as suggested by conventional theory. The authors therefore concluded that in ISEC very high pressures are not only interesting for highly efficient separations (high plate numbers), but also for very fast separations (moderate N values and low t_0 values) of high-MW analytes.

6. Conclusions

Using the kinetic plot method, it has been demonstrated experimentally that columns displaying a difference in kinetic performance under isocratic conditions will display a very similar difference under gradient elution conditions, at least if the columns do not differ too much in retention properties (as is, e.g. the case considering C18-derivatized fully porous and porous-shell particles from different vendors) and are compared under similar mobile-phase composition conditions. This is in agreement with the theoretical expectations, but can only be rigorously demonstrated when comparing the performance in the two elution modes in a maximally unbiased way.

As they offer such an unbiased way, kinetic plots are also ideally suited to for example demonstrate the improved separation performance or gain in analysis time that can be reached when operating at elevated temperature, by being able to be operated at higher pressure, or the advantages of novel particle (e.g. superficially porous particles) or column types (e.g. monolithic columns).

Due to the availability of a very simple set of equations for their construction (cf. Eqs. (3)–(6)), kinetic plot-based comparisons or quality tests can be directly carried out on real experimental data, collected with the sample and mobile phase conditions of one's particular interest.

Acknowledgement

K.B. and D.C. are fellows of the Research Foundation Flanders (FWO Vlaanderen).

Appendix A. Supplementary data

Supplementary data associated with this article can be found, in the online version, at doi:10.1016/j.chroma.2011.08.003.

References

[1] J.C. Giddings, Anal. Chem. 37 (1965) 60.
[2] H. Poppe, J. Chromatogr. A 778 (1997) 3.
[3] X. Wang, D.R. Stoll, P.W. Carr, P.J. Schoenmakers, J. Chromatogr. A 1125 (2006) 177.
[4] F. Lestremau, A. de Villiers, F. Lynen, A. Cooper, R. Szucs, P. Sandra, J. Chromatogr. A 1138 (2007) 120.
[5] G. Desmet, D. Clicq, P. Gzil, Anal. Chem. 77 (2005) 4058.
[6] T. Hara, H. Kobayashi, T. Ikegami, K. Nakanishi, N. Tanaka, Anal. Chem. 78 (2006) 7632.
[7] T.J. Causon, E.F. Hilder, R.A. Shellie, P.R. Haddad, J. Chromatogr. A 1217 (2010) 5057.
[8] P.W. Carr, X. Wang, D.R. Stoll, Anal. Chem. 81 (2009) 5342.
[9] A. de Villiers, F. Lestremau, R. Szucs, S. Gélébart, F. David, P. Sandra, J. Chromatogr. A 1127 (2006) 60.
[10] U.D. Neue, LC·GC Europe 22 (2009) 570.
[11] D. Guillarme, J. Ruta, S. Rudaz, J.-L. Veuthey, Anal. Bioanal. Chem. 397 (2010) 1069.
[12] D. Guillarme, E. Grata, G. Glauser, J.-L. Wolfender, J.-L. Veuthey, S. Rudaz, J. Chromatogr. A 1216 (2009) 3232.
[13] E. Oláh, S. Fekete, J. Fekete, K. Ganzler, J. Chromatogr. A 1217 (2010) 3642.
[14] D.T.-T. Nguyen, D. Guillarme, S. Rudaz, J.-L. Veuthey, J. Chromatogr. A 1128 (2006) 105.
[15] S. Fekete, K. Ganzler, J. Fekete, J. Pharm. Biomed. Anal. 51 (2010) 56.
[16] J. Ruta, D. Guillarme, S. Rudaz, J.-L. Veuthey, J. Sep. Sci. 33 (2010) 2465.
[17] S. Louw, F. Lynen, M. Hanna-Brown, P. Sandra, J. Chromatogr. A 1217 (2010) 514.

[18] A. de Villiers, F. Lynen, P. Sandra, J. Chromatogr. A 1216 (2009) 3431.
[19] A. Fanigliulo, D. Cabooter, G. Bellazzi, B. Allieri, A. Rottigni, G. Desmet, J. Chromatogr. A 1218 (2011) 3351.
[20] J. Billen, G. Desmet, J. Chromatogr. A 1168 (2007) 73.
[21] K. Broeckhoven, D. Cabooter, F. Lynen, P. Sandra, G. Desmet, J. Chromatogr. A 1217 (2010) 2787.
[22] G. Desmet, D. Cabooter, LC·GC Europe 22 (2009) 70.
[23] D.V. McCalley, J. Chromatogr. A 1217 (2010) 858.
[24] G. Desmet, P. Gzil, D. Clicq, LC·GC Europe 7 (2005) 403.
[25] U.D. Neue, D.H. Marchand, L.R. Snyder, J. Chromatogr. A 1111 (2006) 32.
[26] U.D. Neue, H.B. Hewitson, T.E. Wheat, J. Chromatogr. A 1217 (2010) 2179.
[27] S. Eeltink, G. Desmet, G. Vivó-Truyols, G.P. Rozing, P.J. Schoenmakers, W.Th. Kok, J. Chromatogr. A 1104 (2006) 256.
[28] T.J. Causon, E.F. Hilder, R.A. Shellie, P.R. Haddad, J. Chromatogr. A 1217 (2010) 5063.
[29] U.D. Neue, J. Chromatogr. A 1079 (2005) 153.
[30] H. Poppe, J. Paanakker, M. Bronckhorst, J. Chromatogr. 204 (1981) 77.
[31] L.R. Snyder, J.W. Dolan, J.R. Gant, J. Chromatogr. 165 (1979) 3.
[32] L.R. Snyder, D.L. Saunders, J. Chromatogr. Sci. 7 (1969) 195.
[33] F. Svec, J. Chromatogr. A 1228 (2012) 250.
[34] L.R. Snyder, J.W. Dolan, High Performance Gradient Elution, The Practical Application of the Linear-Solvent-Strength Model, Wiley-Interscience, Hoboken, NJ, USA, 2007.
[35] K. Broeckhoven, D. Cabooter, G. Desmet, LC·GC Europe 24 (2011) 396.
[36] D. Cabooter, A. de Villiers, D. Clicq, R. Szucs, P. Sandra, G. Desmet, J. Chromatogr. A 1147 (2007) 183.
[37] A. Fanigliulo, D. Cabooter, G. Bellazzi, D. Tramarin, B. Allieri, A. Rottigni, G. Desmet, J. Sep. Sci. 33 (2010) 3655.
[38] U.D. Neue, J. Chromatogr. A 1184 (2008) 107.
[39] J.J. van Deemter, F.J. Zuiderweg, A. Klinkenberg, Chem. Eng. Sci. 5 (1956) 271.
[40] Y. Zhang, X. Wang, P. Mukherjee, P. Petersson, J. Chromatogr. A 1216 (2009) 4597.
[41] S. Heinisch, G. Desmet, D. Clicq, J.-L. Rocca, J. Chromatogr. A 1203 (2008) 124.
[42] M.M. Fallas, U.D. Neue, M.R. Hadley, D.V. McCalley, J. Chromatogr. A 1209 (2008) 195.
[43] M.M. Fallas, U.D. Neue, M.R. Hadley, D.V. McCalley, J. Chromatogr. A 1217 (2010) 276.
[44] U.D. Neue, C.J. Hudalla, P.C. Iraneta, J. Sep. Sci. 33 (2010) 838.
[45] D. Cabooter, F. Lestremau, A. de Villiers, K. Broeckhoven, F. Lynen, P. Sandra, G. Desmet, J. Chromatogr. A 1216 (2009) 3895.
[46] T. Hara, S. Makino, Y. Watanabe, T. Ikegami, K. Cabrera, B. Smarsly, N. Tanaka, J. Chromatogr. A 1217 (2010) 89.
[47] O. Núñez, K. Nakanishi, N. Tanaka, J. Chromatogr. A 1191 (2008) 231.
[48] K. Miyamoto, T. Hara, H. Kobayashi, H. Morisaka, D. Tokuda, K. Horie, K. Koduki, S. Makino, O. Núñez, C. Yang, T. Kawabe, T. Ikegami, H. Takubo, Y. Ishihama, N. Tanaka, Anal. Chem. 80 (2008) 8741.
[49] S. Miyazaki, M. Takahashi, M. Ohira, H. Terashima, K. Morisato, K. Nakanishi, T. Ikegami, K. Miyabe, N. Tanaka, J. Chromatogr. A 1218 (2011) 1988.
[50] P. Gzil, J. De Smet, G. Desmet, J. Sep. Sci. 29 (2006) 1675.
[51] J. Billen, P. Gzil, G. Desmet, Anal. Chem. 78 (2006) 6191.
[52] T.J. Causon, R.A. Shellie, E.F. Hilder, J. Chromatogr. A 1217 (2010) 3765.
[53] K. Horie, T. Ikegami, K. Hosoya, N. Saad, O. Fiehn, N. Tanaka, J. Chromatogr. A 1164 (2007) 198.
[54] T. Ikegami, K. Horie, N. Saad, K. Hosoya, O. Fiehn, N. Tanaka, Anal. Bioanal. Chem. 391 (2008) 2533.
[55] J. Billen, D. Guillarme, S. Rudaz, J.-L. Veuthey, H. Ritchie, B. Grady, G. Desmet, J. Chromatogr. A 1161 (2007) 224.
[56] P.A. Bristow, J.H. Knox, Chromatographia 10 (1977) 279.
[57] D. Cabooter, J. Billen, H. Terryn, F. Lynen, P. Sandra, G. Desmet, J. Chromatogr. A 1204 (2008) 1.
[58] D. Cabooter, A. Fanigliulo, G. Bellazzi, B. Allieri, A. Rottigni, G. Desmet, J. Chromatogr. A 1217 (2010) 7074.
[59] P.W. Carr, D.R. Stoll, X. Wang, Anal. Chem. 83 (2011) 1890.
[60] G. Desmet, LC·GC Europe 21 (2008) 310.
[61] B. Chauve, D. Guillarme, P. Cléon, J.-L. Veuthey, J. Sep. Sci. 33 (2010) 752.
[62] S. Fekete, K. Ganzler, J. Fekete, J. Pharm. Biomed. Anal. 54 (2011) 482.
[63] H. Kobayashi, T. Ikegami, H. Kimura, T. Hara, D. Tokuda, N. Tanaka, Anal. Sci. 22 (2006) 491.
[64] G. Desmet, D. Cabooter, P. Gzil, H. Verelst, D. Mangelings, Y. Vander Heyden, D. Clicq, J. Chromatogr. A 1130 (2006) 158.
[65] D. Cabooter, S. Heinisch, J.L. Rocca, D. Clicq, G. Desmet, J. Chromatogr. A 1143 (2007) 121.
[66] T.J. Causon, K. Broeckhoven, E.F. Hilder, R.A. Shellie, G. Desmet, S. Eeltink, J. Sep. Sci. 34 (2011) 877.
[67] D. Clicq, S. Heinisch, J.L. Rocca, D. Cabooter, P. Gzil, G. Desmet, J. Chromatogr. A 1146 (2007) 193.
[68] G. Desmet, D. Clicq, P. Gzil, Anal. Chem. 78 (2006) 2150.
[69] H. Xu, S.G. Weber, J. Chromatogr. A 1216 (2009) 1346.
[70] V. Fekete, A. Fekete, J. Fekete, A. Liekens, P. Schmitt-Kopplin, G. Desmet, J. Planar Chromatogr. - Mod. TLC 23 (2010) 440.
[71] J.H. Knox, M. Saleem, J. Chromatogr. Sci. 7 (1969) 614.
[72] J.H. Knox, J. Chromatogr. Sci. 18 (1980) 453.
[73] S.-T. Popovicia, P.J. Schoenmakers, J. Chromatogr. A 1073 (2005) 87.